Field Measurement of Frequency and ROCOF in the Presence of Phase Steps

Paul S. Wright, Peter N. Davis, Kevin Johnstone, Gert Rietveld, *Senior Member, IEEE*, and Andrew J. Roscoe, *Senior Member, IEEE*

***Abstract*— A description of the importance of rate of change of frequency (ROCOF) measurements to the operation of electricity networks is given. The susceptibility of ROCOF measurements to common power system disturbances such as phase steps is described. A measurement campaign to observe ROCOF at multiple locations in an island grid dominated by renewable generation is described and some results are given. These captured ROCOF events are dominated by those associated with phase steps, which occur without significant change to underlying power system frequency. It is concluded that they constitute a "false" ROCOF event. A new algorithm is presented that attempts to remove the influence of the phase step and reduce the associated ROCOF error such that the reliability of ROCOF measurements can be improved in the presence of phase steps. The algorithm is then applied to some recorded waveform sequences from the island that contains phase steps, and the results are presented. In one example, it is shown that a false ROCOF spike in excess of 100 Hz/s was reduced to less than 5 Hz/s.**

***Index Terms*— Frequency measurement, phasor measurement units (PMUs), power system measurements, rate of change of frequency (ROCOF).**

I. Introduction

POWER system frequency and the rate of change of frequency (ROCOF) are key indicators of network stability and of the balance between electricity supply and demand [1], [2]. This balance is becoming more critical with the increased use of highly variable renewable energy sources (RES) for electricity generation.

ROCOF is used as a metric for power system inertia [3] and most commonly to protect networks against the "loss of mains" (LOM) [4]. This situation occurs when power is lost in the wider grid, leaving a section of network operating as an island which is a safety risk of personnel working to restore power. LOM relays use the high levels of ROCOF associated with unsynchronized generation to disconnect this island generation. However, as described in [5], false trips are a common problem with LOM relays due to various network disturbances and due to inadequate quality of the present ROCOF measurements [6]. These false trips have obvious operational and financial consequences for the loss of localized generation and even can cause a cascading loss of generation across the wider network.

This paper describes a measurement campaign to investigate the nature of ROCOF measurements in a high penetration RES distribution network on Bornholm Island, Denmark. The aim of this paper [6] was to capture ROCOF events of the type that could trip LOM relays and examine the cause of any "false" events and their geographical reach. Some results from this ongoing campaign are presented and discussed in Section IV.

Having identified and captured the waveform data, the cause of some of these false ROCOF events was analyzed and categorized, particularly prevalent were those containing "phase steps" [5]. The concept of underlying frequency [7] was then used to design a new algorithm to attempt to remove the phase step, thus reducing the associated ROCOF spike. This algorithm is presented is Section V and associated results when it is applied to some of the Bornholm data are shown in Section VI.

II. ROCOF Measurement Problems

Unfortunately, the measurement of ROCOF is a significant problem with the poor power quality (PQ) waveforms that particularly prevail in low-inertia power networks [3]. This is because an ROCOF measurement first requires frequency to be found using the *d/dt* derivative from phase, before ROCOF is itself determined via a second *d/dt* derivative from frequency. Any noise on the original phase estimate due to poor PQ, transients, fault events, or instrumentation noise are vastly "amplified" by the double derivative, causing spurious results.

RES distributed generators are protected using LOM relays, which trip when the indicated value of ROCOF exceeds a set threshold. However, during imperfect PQ, the spurious noise or ripple uncertainty on ROCOF can be larger than the trip thresholds, resulting in false tripping, for which LOM relays are notorious [4]. These false trips are highly undesirable because they are expensive to the operator and they stress other parts of the grid when major energy sources are disconnected.

Some algorithms for measuring ROCOF are much less tolerant of poor PQ than others. In particular, LOM relays

Manuscript received July 5, 2018; revised September 13, 2018; accepted November 11, 2018. Date of publication December 11, 2018; date of current version May 10, 2019. This work was supported in part by the EMPIR Programme and in part by the Participating States and the European Union's Horizon 2020 Research and Innovation Programme. The Associate Editor coordinating the review process was Michael Lombardi. *(Corresponding author: Paul S. Wright.)*

P. S. Wright and P. N. Davis are with the National Physical Laboratory, Teddington TW11 0LW, U.K. (e-mail: paul.wright@NPL.co.uk).

K. Johnstone and A. J. Roscoe are with the University of Strathclyde, Glasgow G1 1XQ, U.K.

G. Rietveld is with the Van Swinden Laboratorium, 2629 JA Delft, The Netherlands.

Color versions of one or more of the figures in this paper are available online at http://ieeexplore.ieee.org.

Digital Object Identifier 10.1109/TIM.2018.2882907

and phasor measurement units (PMUs) from different manufacturers exhibit very different performance. The PMU instrumentation used to measure ROCOF is the responsibility of the IEEE/IEC joint standards working group 60255-118-1. Due to the on-going difficulties with ROCOF, the committee has relaxed ROCOF compliance requirements during certain tests pending further research to determine algorithms that can operate reliably in representative use case scenarios that exist on power networks [9].

A significant problem with ROCOF measurements is related to phase steps or phase jumps [5]. As the name suggests these are sudden step in phase lasting perhaps a few cycles that do not represent a real change of the power system frequency (see the concept of underlying frequency as developed in [7] and discussed in Section IV). Phase steps have a number of causes including the following.

1) Step change in active power through any inductive component (transformer, overhead line).
2) Fault on one or more phases leading to a phase jump on one or more phases, as active and reactive load currents jump on one (or more) phases.
3) Unbalanced fault which can bring one phase forward and one back, dependent on delta-star and star-delta transformer arrangements.
4) Tap change of a transformer which changes active and reactive loads in a step manner.
5) Switching in or out loads, lines, or generators.
6) Lightning and high-wind storms can cause multiple events of the type above, through direct hits and line clashes, compounded by subsequent protection-system actions.

In the context of ROCOF, phase steps cause spikes in reported ROCOF which easily exceed the trip limits of LOM relays. This amounts to a false trip as the underlying frequency has not changed and the event does not represent a loss of synchronization. This nuisance was of such significance that the U.K. Grid code DC0079 [10] was recently relaxed to reduce the number of false trips caused by phase jumps.

The remainder of this paper examines the measurement of ROCOF in a renewable-rich distribution network on Bornholm Island, Denmark. In Section III describes the measurement configuration and Section IV examines some of the ROCOF event recordings which have resulted from phase steps. An algorithm to attempt to ride-through phase steps is then described, and its performance using Bornholm recorded data is presented.

III. ROCOF Algorithm Testing on Bornholm Island

Bornholm Island is a power network situated in the Baltic Sea with a single interconnection to the Nordic Power Grid, largely capable of independent operation due to its high penetration of RES and an independent diesel power station for periods of low wind generation. Six metrology grade digitizers were installed on the Island in 2016 to conduct PQ research; a full description of the power network and the digitizers is given in [11]. The instrument numbering shown on the plots used below can be linked to instrument location in [11]. These digitizers have the capability of remote reprogramming which allows various ROCOF algorithms to be uploaded and reconfigured.

The six locations were chosen for distributed geographical coverage of the 588-km^2 island, but also for electrical interest. One instrument is located on the island interconnector and measures at the 60-kV levels. A second instrument is connected at 10 kV on the output of a wind farm. The remaining four instruments are at the low-voltage (LV) 440-V level and comprise the two main cities, a rural location and the LV side of the aforementioned wind park, respectively.

All instruments are equipped with GPS which allows accurate time stamping of their measurements. ROCOF algorithms run in real-time and can be configured for various update rates ranging from one reading every 20 ms (50-Hz cycle period) to one reading per 100 ms giving a tradeoff of measurement time latency and noise averaging. The underlying sample rate is adjustable and has a maximum of 30 kS/s. When an ROCOF algorithm on any given instrument measures an absolute value above a preset threshold, a rolling buffer of raw waveform data before and after the trigger event is saved to the local hard disk. This data includes the three voltage and current phases together with detailed GPS timing information. This data can then be downloaded and examined.

Data from an ROCOF trigger event are potentially of significant interest. It could be representative of a real ROCOF event which would be potentially more frequent on a low-inertia network such as Bornholm. Alternatively, it could be a false trigger caused by a PQ disturbance or phase jump such as a switching transient, a voltage dip or swell, or unbalanced fault. Whichever the event, the response of the algorithm with its given configuration will provide valuable information on the limitations of ROCOF such as how PQ events can be rejected, while providing acceptable measurement update rates for real-time power system protection. The ability to replay captured data through alternative algorithms and configurations will be highly advantageous to recommending new normative approaches to ROCOF measurements.

IV. Summary of ROCOF Results

Data have been collected from ROCOF readings around Bornholm from December 2017 onward and a wealth of data exists. ROCOF measurement update rates of 50 Hz have been used for all tests and ROCOF readings above a threshold of 2 Hz/s, in this paper called an ROCOF event, will trigger the recording of waveform data as described above. ROCOF event in the range 2–4 Hz/s occur on average at the rate of about once per day and are regularly seen at the same GPS time on all instruments. Examining the log of results, the results at a given time are mostly of similar value to each other and there is no obvious pattern in which instruments tend to show the biggest or smallest ROCOF.

An example of a recording that seems to show a phase step (to a more lagging phase), followed by a slight increase in underlying frequency, is shown in Fig. 1.

During this time, only four of the six instruments were recording and the event occurred during a time when

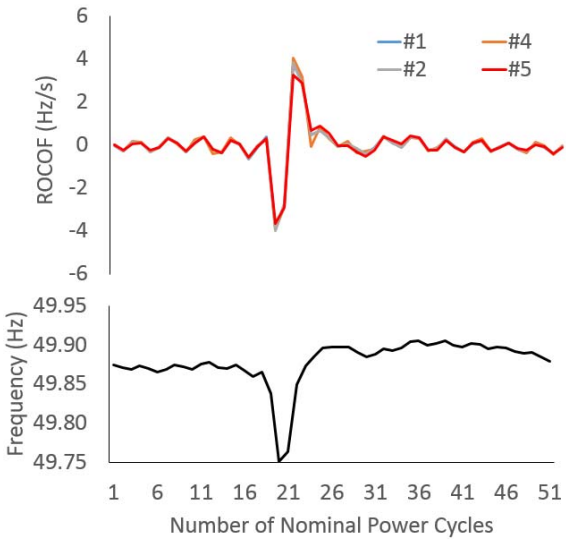

Fig. 1. Recording of an ROCOF event on four instruments on Bornholm on January 1, 2018. Single-dip ROCOF event (top). Measured frequency (only shown for one instrument, the other instrument have similar recordings) (bottom).

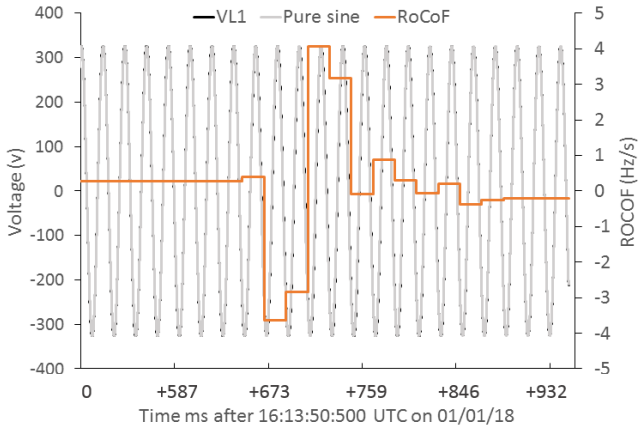

Fig. 2. Time series for ROCOF event shown in Fig. 1 from voltage phase L1 instrument 5 recorded January 1, 2018.

Bornholm is operating in island mode, i.e., disconnected from the Nordic Grid and largely dependent on wind generation. All four instruments record a very similar single-dip ROCOF spike as the measured frequency appears to make step change, before settling to a slightly higher frequency as shown in Fig. 1 (bottom).

The time series recorded on one of the instruments for the L1 voltage at this time is shown in Fig. 2, and there is no visual evidence of any distortion or spikes associated with a fault. Data for phase L1 are plotted (L2 and L3 are similar). A synthesized pure sine wave has been plotted, set to be the same period as the recorded frequency at the start of the sequence. This trace is mostly identical to the VL1 trace at the scale shown in Fig. 2, and it mostly obscures the VL1 trace, however, in the middle section of VL1 can just about be seen emerging from beneath the synthesized plot.

It is possible to zoomed-in view on the traces (not shown here) and it can be seen that the recorded voltage becomes

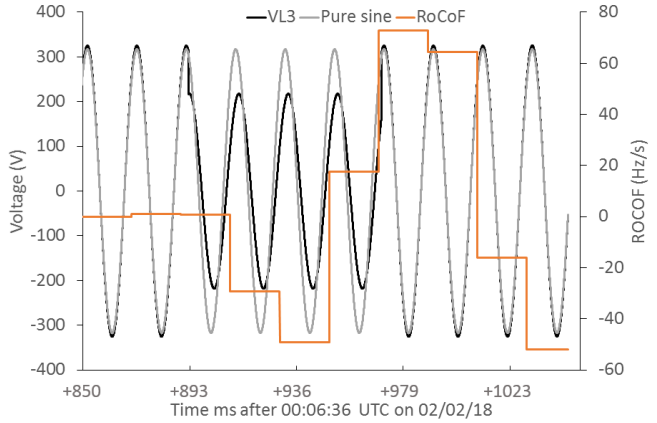

Fig. 3. Phase L3 fault recorded by instrument 1 on Bornholm (February 2, 2018) superimposed on a synthesized sine wave at the underlying frequency. The ROCOF recorded at an update rate of once per cycle.

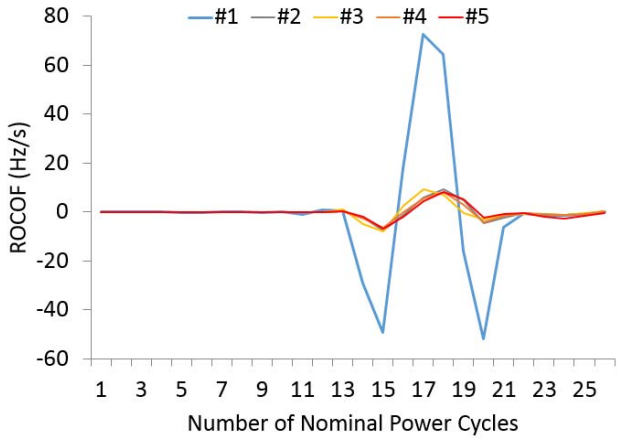

Fig. 4. ROCOF (Roscoe algorithm) recorded at five locations around the Bornholm distribution grid during the four cycle faults (February 2, 2018) recorded in Fig. 3. Note the largest result (1) is the same as the ROCOF plot shown in Fig. 3. Apart from 1, the other traces are similar.

slightly misaligned with the synthesized waveform in the middle of the plot, before returning to largely realign with the underlying frequency. It is possible that the low inertia island network has experienced a negative shift in phase at the point of measurement, perhaps due to a loss of generation, sudden increase of downstream load, or line trip. The nature of the actual situation is unknown.

By far the most common type of event recorded on Bornholm are related to short-lived faults and rather than producing a single-dip frequency pulse as shown in Fig. 1 (ROCOF makes a dip followed by an opposite peak), these events show a dip-peak-dip pulse as shown in Fig. 4. The dip-peak-dip pulse is associated with a phase-step (in the negative direction) followed by a reversal of that phase step to nearly the original phase [7]. Essentially the effect is a dip-peak followed by a peak-dip, but when the fault is short and commensurate with the filter window used to measure ROCOF, the dip-peak–peak-dip merges to a dip-peak-dip, with the area under the central peak equal to the total area of the two dips.

Phase steps are prevalent in networks for a variety of reasons as described above; from the results of various ROCOF

events captured on Bornholm, many are caused by short-lived faults of the order of four cycles in length which occur typically several times per week. These faults are typified by a significant dip in voltage on one of the three phases and associated lesser disturbance on the other phases.

A plot of a fault of this nature is shown in Fig. 3 for phase L3 as recorded by instrument 1 on Bornholm. It can be seen that a fault has occurred that starts in the third cycle which lasts until the seventh cycle. Fig. 3 shows a simulated pure sine wave at a frequency set to that recorded prior to the fault. It can be seen that during the fourth cycle fault, the phase of L3 has a small (just visible) phase shift to the right compared with the pure sine wave. Following the fault, this phase shift recovers and the recorded L3 voltage recovers most of the phase step to realign with the underlying phase of the pure sine wave.

The term underlying phase also implies an underlying frequency and ROCOF. The alternative signal model which introduced these concepts is defined in [7] and is expressed as follows (reproduced from [7, eq. (4)]):

$$x(t) = X_m(t)\cos(\theta(t) + \varphi(t)). \tag{1}$$

Here, the underlying phase is defined by $\theta(t)$ and phase $\varphi(t)$ which contains the information on the phase step. In power networks, it is more useful to consider the underlying frequency ω which is related to underlying phase $\theta(t)$ by ω multiplied by time t.

Fig. 3 shows the ROCOF as recorded using an adaptive filters PMU algorithm [8] at an update rate of 50 Hz. It can be seen that fault has registered a considerable ROCOF spike of some 70 Hz/s. There is a marginal indication of a change in phase after the fault relative to the phase before the fault. This can be seen by carefully looking at cycles 8 and 9 in Fig. 3 which show that the recorded voltage is no longer visually coincident with the simulated pure sine. This is an example of a change in the underlying phase $\theta(t)$ (1) typical of the changing frequency in a power system. However, the size of recorded ROCOF is largely misleading and can be mostly represented by the phase step term $\varphi(t)$ in (1).

Recordings of ROCOF around Bornholm during this fault further support the assumption that Fig. 3 is dominated by phase steps, and the metric of interest for power system control is the ROCOF analysis of the underlying frequency. Fig. 4 shows ROCOF recorded at all six sites around the Bornholm network during the event, with the largest plot registered on instrument 1, i.e., the same results as shown for ROCOF in Fig. 3. The other sites in the distribution system also register the fault, but the recorded ROCOF is much reduced to less than 10 Hz/s in all five other cases. The assumption is that instrument 1 is close to the fault and the effects of the fault are reduced at the other measurement sites. The larger measured ROCOF at one site, is likely due to the change in active and reactive currents caused by the fault and the changes nearer the fault would be more pronounced.

If the instrument 1 result was a meaningful ROCOF of 70 Hz/s in the sense that there had been a wide-area shift in power system phase and frequency, then it would be expected that the other Bornholm sites would have recorded similar sized ROCOF values. It is, therefore, assumed that the fault has contributed a large phase step $\varphi(t)$ which is typified by the dip-peak-dip ROCOF response in Fig. 4. The first half (the dip-peak) is caused by the step in phase $\varphi(t)$ and the second half (peak-dip) four cycles later by its recovery to the underlying phase. The other sites exhibit the same shaped response, but in these cases $\varphi(t)$ is smaller.

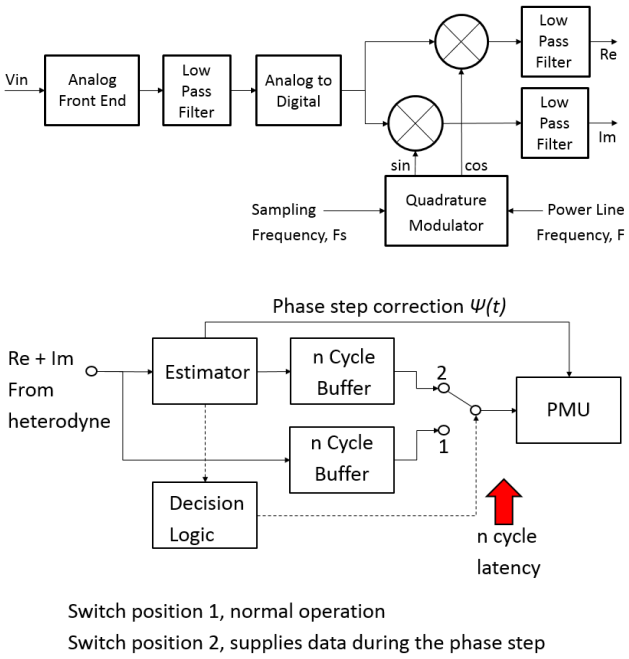

Fig. 5. Proposed scheme for phase step removal.

Bornholm is dominated by wind generation and if ROCOF-based LOM relays were used to protect these installations, then this fault would have likely caused considerable false relay tripping with high impact on the distribution network. In this context, it is instructive to consider ROCOF LOM protection as governed in U.K. grid code DC0079 [10] which specifies the ROCOF measurement update rate to be 500 ms (compared to the 20 ms as used in Fig. 4). Slower update rates have the effect of reducing ROCOF and when Fig. 4 data is analyzed using a 500-ms update rate it reduces the ROCOF spike result to a peak of about 1.5 Hz/s. However, this is still larger than the 1-Hz/s trip threshold as specified in the U.K. grid code and the phase-step recorded in Fig. 4 would exceed the threshold causing the wind park close to instrument 1 to trip off the network.

An algorithm where the $\varphi(t)$ phase step term can be identified and removed from (1) would allow the ROCOF resulting from the underlying frequency to be measured thus affording LOM protection and reducing false trips.

V. Algorithm to Measure Underlying Frequency and ROCOF in the Presence of Phase Steps

Working on the premise that the objective of an ROCOF instrument is to measure the underlying frequency and underlying ROCOF, then a system to remove the influence of phase steps $\varphi(t)$ is required. A proposed scheme for phase step removal is depicted in Fig. 5.

The algorithm uses the real (Re) and imaginary (Im) parts output from the heterodyne modulator employed in the PMU algorithm [9] shown in Fig. 5 (top), provided at the PMU sampling rate. Conventionally, these Re and Im data from each line-phase are fed to the chosen PMU algorithm which contains digital filters, positive sequence calculations, and a data decimator.

When the switch in Fig. 5 is at position 1, this conventional data processing method is used as normal with the exception that the data are delayed in a first-in first-out (FIFO) buffer by n-cycles. This n-cycle latency is added to give sufficient time to process data to decide whether a phase step has occurred. For example, the typical fourth-cycle phase steps commonly seen on Bornholm should be identified and removed during this latency period.

When a suspected phase step occurs, the FIFO provides an n-cycle period in which it has to be decided whether the data is an actual valid ROCOF event or a short-lived phase step. In the case of an actual phase change [i.e., a change to the underlying phase $\theta(t)$], the decision logic will not change the switch from position 1 and the data will continue uninterrupted and will be processed as normal.

However, in the case of a phase step $\varphi(t)$, the incoming data is replaced with an estimation of the Re and Im result of the heterodyne process for only the assumed underlying signal

$$x(t) = X_m(t)\cos(\theta(t)). \tag{2}$$

The estimated signal is required in order to maintain an uninterrupted stream of Re and Im data to the PMU algorithm. Continuous data is essential because the PMU consists of digital filters and interrupting the data stream to the algorithm will in itself cause discontinuities resulting in ROCOF spikes.

In order to synthesize the replacement data, an estimator of the signal dynamics is required to model the underlying signal during a phase step. The replacement data estimator will run continuously, even when there are no suspected issues with the data, and is required to track the phase, amplitude and frequency of the real data. In a real power system, these parameters are all time varying and the accuracy of the estimator will ultimately determine how well the effect of the phase step can be removed from the PMU output. It should also be remembered that the estimator must run in real time and must, therefore, be computationally efficient. The output of the estimator is fed into an indicial n-cycle FIFO buffer to that used in switch path 1.

If the decision logic judges the data to contain a phase step, the switch is changed to position 2 to provide the estimated data to the PMU until such time as the phase step is deemed to be over. At the conclusion of the phase step, the switch is changed back to position 1 to provide the real data again.

The process of the changeover of the switch is likely to introduce discontinuities due to the differences between the real and estimated data, which in turn will give rise to erroneous ROCOF steps on the PMU. Ensuring a smooth changeover between the two step positions requires an accurate estimator whose data is in phase with the real data. Data changeover is one of the main challenges of this method and a period of estimator alignment to the real data following the end of a phase step is likely to be needed to minimize errors.

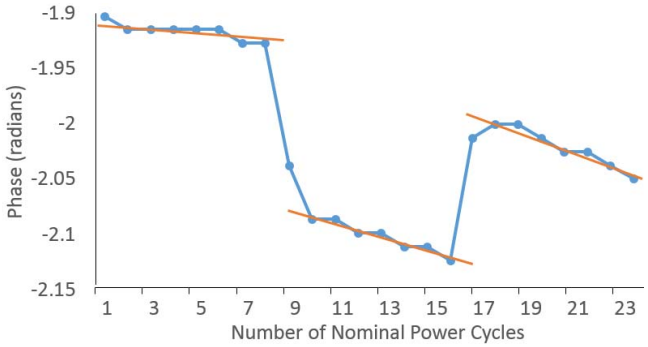

Fig. 6. Trajectory of the phase updated once per half cycle, as shown by the marker points, for a Bornholm recording January 9, 2018. Straight lines: approximate to the trajectories of the sections (these are added schematically rather than by use of linear regression).

VI. Implementation and Results

The estimator model is based on a least-squares trajectory estimation of the fundamental phase and the magnitude of the real data. The complexity of the estimator is a tradeoff of accuracy versus computational time and as such this simple estimator does not attempt to add harmonics to match those in the real signal.

The estimator is fed with the incoming Re and Im data. Once the estimator is settled, its output can be used as a comparison with further incoming data to look for departures from the expected trajectory and act as a trigger for a potential phase step. Upon triggering of an event, the estimator no longer uses the incoming data to update itself but maintains the trajectory that prevailed prior to the event, thus supplying data to the PMU reflecting the underlying trend.

Also upon identification of an event, a second parallel estimator is started taking inputs from the incoming data. This attempts to find a settled plateau of a possible phase jump.

Ideally, the algorithm works as shown in Fig. 6 which shows a plot of phase (in radians) versus time with data points updated once every half nominal power cycle. The estimated trajectory in the first of the three sections is used to replace data in the second section, until that trajectory has been confirmed as stable. These two functions can be used to determine the phase step size $\varphi(t)$, as in some cases the phase step could be permanent or long lived and the value could be used to back off the phase step and avoid a large ROCOF spike.

In the case of Fig. 6, the more typical case is shown where the phase step reverses and the third section shows this step back. What is particularly challenging in this case is that the second and third section slopes show an actual change in trajectory compared to the first section slope. So there is likely to be some actual frequency change occurring as the power system responds to the fault that caused the phase step. It is the effect of the phase step that needs to be removed, but the actual phase trajectory change must be kept so that the instrument correctly records the underlying frequency.

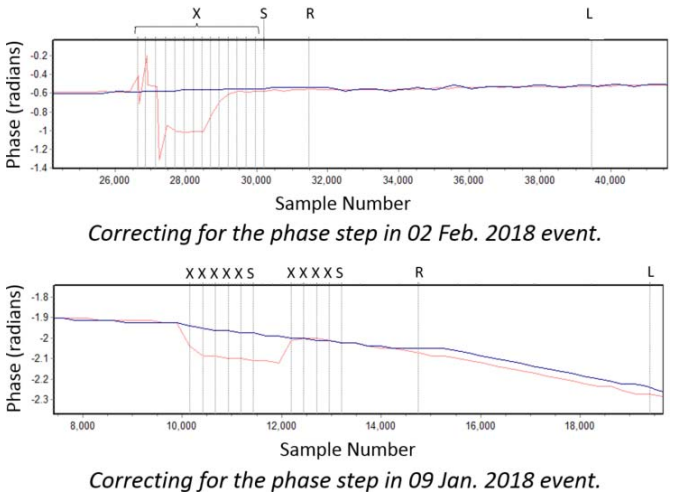

Fig. 7. Measured phase of two Bornholm events (shown by the discontinuous line) clearly showing the phase step. Smoother line: phase step correction by the proposed algorithm. The "X," "S," and "R" markers show the various stages of the algorithm operation. The sampling rate is 25.6 kS/s.

Attempting to back out the phase step is very challenging in the case of Fig. 6, and the estimation of the trajectory in the second section is an important element of this. Incorrect size back out or removal will cause its own spike in the ROCOF.

It has been pointed out that an algorithm such that uses the trajectory is typical of what is called operationalist measurement [12], where a change in the choice of algorithm will give a change in the result, such that the method will only give repeatable results if the procedure (or "operation") is exactly followed. If a trajectory-based algorithm can be developed and optimized to back-out phase steps, it will do so in the absence of suitable mathematical procedure to describe frequency during a phase jump. Once a suitable algorithm is optimized, it may be possible to prescribe it as an operationalist solution.

A proposed operationalist solution in the form of a trajectory-based algorithm was attempted as shown in Fig. 7, which shows the phase at the input (the output of the heterodyne) sampled regularly once per nominal power cycle plotted against time. Plots are shown for two recorded cases of phase steps in Bornholm; case 020218 which has a phase step with a relatively constant underlying frequency and the above Fig. 6 case 090118 which contains a phase step and a changing underlying frequency.

The discontinuous trace in Fig. 7 line shows the phase of input data, and the smoother trace shows the corrected phase result from the algorithm. Data marked with "X" indicates that a phase disturbance has been detected and the algorithm is processing the change and providing extrapolated data using the phase trajectory prior to the disturbance. The "S" mark indicates that the algorithm has settled on a new stable phase trajectory and the size of any remaining phase step can then be calculated. The "R" mark indicates that real data is again being used (returned to switch position 1) with any phase step backed out.

It can be seen from Fig. 7 (top) that the algorithm has correctly extrapolated the trajectory of the phase through the 020218 fault. The phase step is relatively short and steps back to near its original level before the algorithm has settled on the lower part of the step. So the "X" marks continue to appear through the step, showing that the algorithm is continuously extrapolating beyond the return of the step when finally at "R," the algorithm has settled. So in this case no backing out of this short phase step has occurred, rather it has been removed by extrapolation. After the "S" point, the gain of the estimator drives its phase toward that of the real data closing the small offset, until it is aligned at "R" when the real data is used again as an input to the PMU.

In contrast, Fig. 7 (bottom) shows the 090118 case where a phase step is backed out. In this case, the phase step is of a similar length in time to the upper plot, but has less of a perturbation such that the algorithm is able to settle at point "S" near the middle of the phase step. At this point, the estimator stops extrapolating and updates itself with new real data, however, the PMU is still fed with the estimator data, rather than restored raw real data. The reason for this is that the estimator has started aligning with the real data phase, only to be again disturbed by the phase stepping back to its original trajectory near the next "X." The settling process then repeats until finally at "R" the real data can be restored. After this point there is a small constant offset in the phases, this is due to an error in the two phase step back out's that occurred at the "S" points. This constant phase offset is of no consequence to ROCOF measurements (the differential of a constant phase is zero), but can be slowly removed by the estimator if necessary.

The output phase data shown in Fig. 7 are applied to the C37 standard PMU algorithm to calculate ROCOF.

Fig. 8 shows the resulting ROCOF plotted against measurement number, updating once every 20 ms. The three traces are the results of processing the various data streams through the standard PMU algorithm for the simpler 020218 case [Fig. 7 (top)]. The uncorrected ROCOF is shown by the blue plot and for plotting clarity it is shown clipped at ± 25 Hz/s, whereas the measured maximum is some 107 Hz/s. The "estimator" plot is the result of running only the estimator output through the standard ROCOF algorithm. During the fault event which starts at the x-axis point 43, this data becomes more noisy as the estimator starts to extrapolate the data in the absence of real data (corresponding to the points marked "x" in Fig. 7). At the end of the fault the real data again starts (corresponding to point "r"), conditioning the estimator which settles back to a noise pattern similar to before the fault.

The dotted "substitution" plot is a mixture of interleaved real and estimator data, with the estimated data replacing the real during the phase step. It can be seen that the dotted plot is identical to the input "original" plot up to result 42 on the x-axis as the PMU is fed with the uncorrected input data. At result 43, the estimated data is substituted, replacing the real data until result 54 when the real data is returned. The noise during the fault period (x-axis result 44 to 53) is similar to the pure estimator data, it being the same data during this period. Real data are switched back to the PMU input at result 54 and a small spike in ROCOF value results of some ± 3 Hz/s; this is most likely to be caused by a misalignment of the estimator

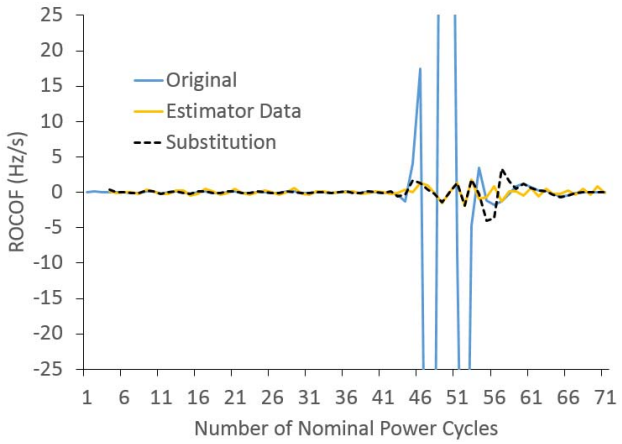

Fig. 8. ROCOF for the 020218 case. The "original" trace shows the uncorrected measured ROCOF clipped at ±25 Hz/s (unclipped maximum 107 Hz/s). When the output of the synthesizer data only is used, the "estimator" trace shows the resulting ROCOF. The dotted trace is a mixture of the two (see text).

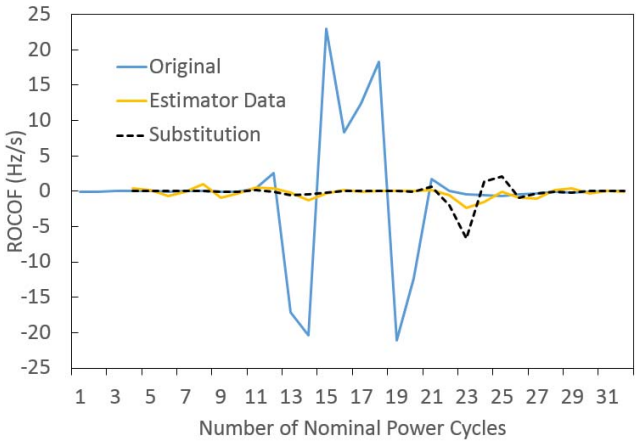

Fig. 9. ROCOF for 090118 case (uncorrected ROCOF max = 22 Hz/s). The "original" trace shows the uncorrected measured ROCOF. When the output of the synthesizer data only is used, the "estimator" trace shows the resulting ROCOF. The change-over data when the real data is substituted during the fault is shown by the dotted plot.

and the real data injecting a small phase step in to the ROCOF algorithm at the point of data switch over at time 54 on the x-axis of Fig. 8. The ROCOF algorithm clearly takes some time to settle after this perturbation.

Fig. 9 shows the results for the other 090118 case which contains a phase step and in addition a change in underlying frequency. In this case at the point of change back to real data at result 22, the ROCOF of the dotted plot shows a similar perturbation to that of Fig. 8 case. Low-noise data is achieved in the middle of the phase step between point 16 and 20 in Fig. 9, since the estimator is not extrapolating at this time (see the first point "S" in the lower Fig. 7 plot), but being trained by the real data.

VII. Conclusion

Phase steps are a significant source of error in ROCOF measurements, assuming the objective is to measure the underlying frequency and underlying ROCOF. When ROCOF LOM relays are used to protect renewable power parks, phase steps become a major cause of false trips causing loss of revenue and undermining the stability of the power system.

ROCOF measurements on Bornholm Island show that significant fault-related phase steps occur on average several times per week. The multiple-site measurements assumed to be close to a fault show levels of ROCOF that are greater than at more distant sites, which supports the concept of underlying frequency and emphasizes the need to remove the influence of the phase step to determine the underlying trends.

The new method of phase step removal presented here is reasonably successful in removing the phase steps. In the case of a low underlying ROCOF (assumed to be close to 0 Hz/s), the phase step spike was reduced from a peak of 107 Hz/s to a peak of about 3 Hz/s. In the case of a changing underlying frequency and phase step, the improvement is not so good, reducing the ROCOF spike peak from about 25 to about 6 Hz/s. As already pointed out with this proposed operationalist solution, changing the algorithm parameters, will change the output and both results presented here are sensitive to algorithm configuration. The reported results should be considered an indication of what can be achieved with this method. It is possible that the method can be improved by using superior estimators and particularly better alignment of the estimator to the real data at switch over; the ROCOF algorithm being extremely sensitive to any phase step introduced at the point of switching from real data to estimator data and vice versa.

Currently, the algorithm is running on a desktop PC using recorded fault data from Bornholm Island. More work is required to implement the algorithm into the Bornholm instruments for real-time operation. Further testing with other common PQ issues is also required to check for malfunctions and instabilities.

The algorithm also increases latency (the delay lines) and as is common, there is a tradeoff between latency and peak reduction. In this paper, latency is set at five cycles.

Acknowledgment

The authors would like to thank A. Christensen of Trescal DK and Lars and P. Sonne-Pedersen from Energetic Bornholm for their technical support on the Bornholm measurement campaign.

References

[1] P. Wall *et al.*, "Smart frequency control for the future GB power system," in *Proc. IEEE Innov. Smart Grid Technol. Eur. (ISGT-Europe)*, Oct. 2016, pp. 1–6.

[2] National Grid, U.K. (2016). *Enhanced Frequency Control Capability (EFCC) Project*. Accessed: May 2018. [Online]. Available: https://www.nationalgrid.com/uk/investment-and-innovation/innovation/system-operator-innovation/enhanced-frequency-control

[3] Q. Gao and R. Preece, "Improving frequency stability in low inertia power systems using synthetic inertia from wind turbines," in *Proc. IEEE Manchester PowerTech Conf.*, Jun. 2017, pp. 1–6.

[4] C. F. Ten and P. A. Crossley, "Evaluation of ROCOF relay performances on networks with distributed generation," in *Proc. IET 9th Int. Conf. Develop. Power Syst. Protection*, 2008, pp. 523–528.

[5] A. Riepnieks, H. Kirkham, A. J. Faris, and M. Engels, "Phase jumps in PMU signal generators," in *Proc. IEEE PES Gen. Meeting*, Chicago, IL, USA, Jul. 2017, pp. 1–5.

[6] P. S. Wright, P. N. Davis, K. Johnstone, G. Rietveld, and A. J. Roscoe, "Field testing of ROCOF algorithms in multiple locations on Bornholm Island," in *Proc. CPEM*, Paris, France, 2018, pp. 1–2.
[7] A. J. Roscoe, A. Dyśko, B. Marshall, M. Lee, H. Kirkham, and G. Rietveld, "The case for redefinition of frequency and ROCOF to account for AC power system phase steps," in *Proc. IEEE Int. Workshop Appl. Meas. Power Syst. (AMPS)*, Sep. 2017, pp. 1–6.
[8] A. J. Roscoe, I. F. Abdulhadi, and G. M. Burt, "P and M class phasor measurement unit algorithms using adaptive cascaded filters," *IEEE Trans. Power Del.*, vol. 28, no. 3, pp. 1447–1459, Jul. 2013.
[9] *IEEE Standard for Synchrophasor Measurements for Power Systems—Amendment 1: Modification of Selected Performance Requirements*, IEEE Standard C37.118.1a-2014, 2014.
[10] (Dec. 15, 2017). *UK Distribution Code: DC0079—Frequency Changes during Large Disturbances and their Impact on the Total System*. Accessed: May 14, 2018. [Online]. Available: http://www.dcode.org.uk/assets/uploads/DC0079_Ofgem_Decision.pdf
[11] P. S. Wright, A. E. Christensen, P. N. Davis, and T. Lippert, "Multiple-site amplitude and phase measurements of harmonics for analysis of harmonic propagation on Bornholm Island," *IEEE Trans. Instrum. Meas.*, vol. 66, no. 6, pp. 1176–1183, Jun. 2017.
[12] *Operationalization*. Accessed: Sep. 12, 2018. [Online]. Available: https://en.wikipedia.org/wiki/Operationalization

Paul S. Wright received the B.Sc. and Ph.D. degrees in electrical and electronic engineering from the University of Surrey, Surrey, U.K., in 1987 and 2002, respectively.

He spent three years as a Research Fellow with the University of Surrey, where he was involved in the field of spacecraft sensors and attitude control. This was followed by three years with the Central Electricity Research Laboratory, Leatherhead, U.K., where he was involved in advanced control systems. In 1992, he joined the National Physical Laboratory, Teddington, U.K., where he is currently a Principle Research Scientist specializing in ac measurements and waveform analysis. He is a coordinator of the EU project on ROCOF of which this work is part.

Peter N. Davis received the M.Phys. degree from the University of York, York, U.K., in 2009, and the Fd.Eng. degree in electrical power engineering from the University of Aston, Birmingham, U.K., in 2013.

He spent a brief period working in local government before joining National Grid Warwick, U.K., in 2011 on an engineering training scheme. In 2013, he joined the National Physical Laboratory, Teddington, U.K., where he is currently a Senior Research Scientist.

Kevin Johnstone received the M.Eng. degree in aero-mechanical engineering from the University of Strathclyde, Glasgow, U.K., in 2009, where he is currently pursuing the Ph.D. degree with a focus on the simulation of transient stability phenomena in U.K. resulting from increased wind power penetration and wind power control methods for mitigating these issues.

He worked as an Engineer for Airbus U.K., Bristol, U.K., for two years. He is currently a Research Assistant in advanced electrical systems with the University of Strathclyde, with a focus on smart grid simulation and control.

Gert Rietveld (M'10–SM'12) received the M.Sc. (*cum laude*) and Ph.D. degrees in low-temperature and solid-state physics from the Delft University of Technology, Delft, The Netherlands, in 1988 and 1993, respectively.

In 1993, he joined the Van Swinden Laboratorium, Delft, where he is currently the Chief Metrologist. His current research interests include breadth of electromagnetic precision measurements, focusing on power and high-voltage metrology and smart electrical grids.

Dr. Rietveld is a Member of the International Committee for Weights and Measures and the President of its Consultative Committee for Electricity and Magnetism (CCEM). He is also the Chair of the Energy Task Group of the European Association of the National Metrology Institutes (EURAMET), the Founding Chair of the EURAMET Subcommittee on Power and Energy, and a Member of several CCEM, EURAMET, CIGRE, and IEEE Working Groups.

Andrew J. Roscoe (M'13–SM'15) received the B.A. and M.A. degrees in electrical and information sciences tripos from Pembroke College, Cambridge, U.K., in 1991 and 1994, respectively.

From 1991 to 1995, he was with GEC Marconi, Chelmsford, U.K., where he was involved in antenna design and calibration, specializing in millimeter-wave systems, and solid-state phased-array radars. From 1995 to 2003, he was with Hewlett Packard South Queensferry, U.K., and subsequently Agilent Technologies, Santa Rosa, CA, USA, in the field of microwave communication systems, specializing in the design of test and measurement systems for personal mobile and satellite communications. Since 2004, he has been with the University of Strathclyde, Glasgow, U.K., where he is invloved in power systems. His current research interests include power system measurement algorithms, marine power systems, laboratory demonstration with power-hardware-in-the loop capability, and the integration of high penetrations of converter-connected renewables.